

Report

R-23-12

November 2023



Assessment of heterogeneous processes and parameters to be used in models for radiation induced dissolution of spent nuclear fuel

Mats Jonsson

SVENSK KÄRNBRÄNSLEHANTERING AB

SWEDISH NUCLEAR FUEL
AND WASTE MANAGEMENT CO

Box 3091, SE-169 03 Solna
Phone +46 8 459 84 00
skb.se

SVENSK KÄRNBRÄNSLEHANTERING

ISSN 1402-3091

SKB R-23-12

ID 2015434

November 2023

Assessment of heterogeneous processes and parameters to be used in models for radiation induced dissolution of spent nuclear fuel

Mats Jonsson

KTH Royal Institute of Technology, Department of Chemistry

Keywords: Radiolysis, Surface reactions, Kinetics, Spent nuclear fuel, Numerical models.

This report concerns a study which was conducted for Svensk Kärnbränslehantering AB (SKB). The conclusions and viewpoints presented in the report are those of the author. SKB may draw modified conclusions, based on additional literature sources and/or expert opinions.

This report is published on www.skb.se

© 2023 Svensk Kärnbränslehantering AB

Abstract

In this work, surface reaction mechanisms and the corresponding kinetic parameters for processes relevant when designing numerical models to predict the dynamics of radiation induced dissolution of UO₂-based spent nuclear fuel are presented and summarized. The implementation of some of the heterogeneous features of the system into a numerical model accounting for both homogeneous and heterogeneous processes is also discussed. In addition, the steady-state approach for modelling of spent nuclear fuel dissolution is described as a proposed benchmarking model. Finally, a discussion on current knowledge gaps of key-importance for the development of numerical models is included.

Sammanfattning

I detta arbete har ytreaktionsmekanismer med tillhörande kinetiska parametrar för processer av relevans vid utveckling av numeriska modeller som beskriver dynamiken för strålningsinducerad upplösning av UO_2 -baserat utbränt kärnbränsle presenterats och sammanfattats. I arbetet diskuteras också hur de heterogena processerna enklast kan inkluderas i en modell som både beskriver homogena och heterogena processer. Den tidigare utvecklade ”steady-state”-modellen för upplösning av utbränt kärnbränsle beskrivs också och föreslås användas som referensmodell vid utveckling av nya modeller. Slutligen diskuteras aktuella kunskapsluckor som anses kritiska vid modellutveckling.

Contents

1	Introduction	7
2	The mechanism of radiation induced dissolution of UO₂ based spent nuclear fuel	9
2.1	Radiolysis of water	10
2.2	Kinetics of surface reactions	10
2.3	Oxidation of UO ₂ by radiolytic oxidants	11
2.4	Dissolution of oxidized UO ₂	11
2.5	The relative impact of radiolytic oxidants	11
2.6	The mechanism of the reaction between H ₂ O ₂ and UO ₂	12
2.7	The effect of H ₂	12
2.8	Other reactions catalyzed by ε-particles	13
3	The steady-state approach	15
4	Reactions and rate constants	17
4.1	H ₂ O ₂ + UO ₂	17
4.2	HCO ₃ ⁻ facilitated dissolution of UO ₂ ²⁺	17
4.3	H ₂ O ₂ + UO ₂ catalyzed by ε-particles	18
4.4	The interfacial H ₂ effect	18
4.5	O ₂ + UO ₂	18
4.6	O ₂ + UO ₂ catalyzed by ε-particles	19
4.7	Other reactions catalyzed by ε-particles	19
4.8	Reactions of ·OH and CO ₃ ⁻ with UO ₂	19
4.9	Summary of reactions and rate constants	20
5	Known unknowns	21
5.1	Transferring kinetics from powder to pellet	21
5.2	Extended exposure	21
5.3	Secondary phases	21
5.4	Speciation in solution	21
5.5	Kinetic expressions based on adsorption isotherms	22
5.6	Impact of interfacial G-values	22
5.7	Surface reactivity of reducing radicals	22
	References	23

1 Introduction

Numerical modeling of radiation induced dissolution of spent nuclear fuel is a key-component of safety assessments of geological repositories for spent nuclear fuel. A reliable model must be based on well-established mechanistic knowledge and verified rate constants in combination with a code capable of handling the heterogeneous nature of the system. The processes that must be accounted for are (1) radiation chemistry of water, (2) surface reactions between aqueous radiolysis products and the fuel surface, (3) dissolution, adsorption and precipitation of secondary phases and (4) diffusion.

The general approach when accounting for all the features above is to divide the solution in small volume elements. The radiation chemistry is treated homogeneously in each volume element in parallel with the diffusion between the volume elements. In the innermost volume element (closest to the surface), the surface reactions are handled together with the homogeneous radiation chemistry.

In addition to these processes, it is essential that the spatial dose rate distribution is correctly described. Recently, the reactions, rate constants and radiation chemical yields (G-values) for water radiolysis were reviewed with the purpose of identifying the most suitable set of reactions and parameters to be included in a numerical model (Jonsson 2022). In this report, the heterogeneous processes and parameters relevant for modeling radiation induced dissolution of spent nuclear fuel are reviewed.

2 The mechanism of radiation induced dissolution of UO_2 based spent nuclear fuel

Radiolysis of water produces oxidants that are capable of oxidizing the UO_2 -matrix and thereby facilitate its dissolution (Shoesmith 2000). The dissolution of oxidized UO_2 is further facilitated by the presence of $\text{HCO}_3^-/\text{CO}_3^{2-}$ in the groundwater (Grenthe et al. 1984, de Pablo et al. 1999). In the absence, or at very low concentrations, of $\text{HCO}_3^-/\text{CO}_3^{2-}$ secondary phase formation on the fuel surface can occur. This would in general reduce the rate of oxidative matrix dissolution. In figure 2-1, the most important reactions involved in radiation induced oxidative dissolution of UO_2 based spent nuclear fuel are given.

In the following text, these reactions are discussed individually.

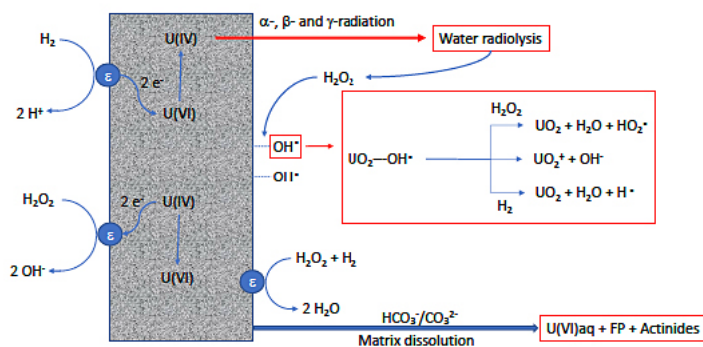


Figure 2-1. General mechanism for radiation-induced oxidative dissolution of UO_2 -based nuclear fuel in water.

2.1 Radiolysis of water

Upon absorption of ionizing radiation, water undergoes ionization and excitation (Spinks and Woods 1990). Initially, these events are highly localized but within less than 10^{-6} s the initially formed species have fragmented and some of the reactive fragments have recombined into molecular species at the same time as they have diffused out from where they were originally formed. At this point, we can consider the irradiated volume to be more or less homogeneous provided that there are no dose rate gradients. The irradiated volume will contain oxidants (HO^\bullet , HO_2^\bullet and H_2O_2) as well as reductants (e_{aq}^- , H^\bullet and H_2). The yields of these products are referred to as radiation chemical yields or G-values and they are expressed as the amount of a given species produced or consumed per unit of absorbed radiation energy. The SI-unit is mol J^{-1} but the older unit molecules per 100 eV is still frequently used. The radiation chemical yield in a given absorber depends on the type of radiation as well as on the radiation energy.

Under the conditions considered relevant for the safety assessment of a geological repository for spent nuclear fuel, the radiation chemistry in the vicinity of the fuel surface will be dominated by alpha-radiation. The G-values for alpha-radiolysis and the relevant reactions and rate constants in water and water containing $\text{HCO}_3^-/\text{CO}_3^{2-}$ have recently been reviewed (Jonsson 2022) and will not be further discussed here.

2.2 Kinetics of surface reactions

Oxidative dissolution of UO_2 involves oxidation of UO_2 by radiolytic oxidants formed in solution. In a very simple fashion, this can be seen as the interfacial equivalent of a bimolecular process. In homogeneous systems, the rate expression for a bimolecular elementary reaction (e.g., $\text{A} + \text{B} \rightarrow \text{Product}$) is given by:

$$-\frac{d[A]}{dt} = k[A][B] \quad (2-1)$$

Where k is the rate constant and $[A]$ and $[B]$ are the concentrations of the reactants A and B, respectively.

For a surface reaction in an aqueous system (e.g., $\text{A}(\text{aq}) + \text{B}(\text{s}) \rightarrow \text{Product}$) we could use the following expression (Jonsson 2010):

$$-\frac{d[A]}{dt} = k[A] \frac{SA}{V} \quad (2-2)$$

In this case, the reactive surface is quantified by the solid surface area (SA) to solution volume (V) ratio. In the homogeneous system the rate constant has the unit $\text{M}^{-1} \text{s}^{-1}$ and the limit for diffusion control, i.e., the rate constant for a reaction with no activation barrier (where every collision will result in reaction), is usually around $10^{10} \text{M}^{-1} \text{s}^{-1}$ in aqueous solution at room temperature. For a surface reaction expressed as above, the unit of the rate constant is m s^{-1} and the limit for diffusion control depends on the dimensions of a solid (Jonsson 2010). In general, the limit for diffusion control in a heterogeneous system is much lower than for homogeneous systems. The limit for diffusion control decreases with increasing solid particle size. Although it would be desirable to quantify the reactive surface in terms of reactive sites, experiments usually only allow for the use of solid surface area to solution volume ratio. If the reactive site density of the solid material is known, rate constant derived from the above relationship can easily be converted and the unit would then be the same as for the homogeneous system. A UO_2 surface site density of $2.1 \times 10^{-4} \text{mol} \cdot \text{m}^{-2}$ has been derived in the work of Hossain and Jonsson (Hossain and Jonsson 2008). Surface site concentrations can be expressed using the $S \cdot V^{-1}$ ratio in combination with the surface site density.

The second order rate constant for a surface reaction can be determined by monitoring the concentration of the solute reactant as a function of time in a system where the solid surface is present in excess. The reaction order would then be 1 and we can determine a pseudo first order rate constant for these specific conditions. By performing the experiment at different solid surface area to solution volume ratios, always with an excess of surface, the second order rate constant can be determined by plotting the pseudo first order rate constant as a function of solid surface area to solution volume ratio (the slope of the plot) (Jonsson 2010).

When performing numerical simulations including surface reactions it is important to keep in mind that the surface reaction should only be accounted for in the volume element closest to the surface and that the solid surface area to solution volume ratio refers to the volume of the innermost volume element, not the whole system (Nielsen and Jonsson 2008, Nielsen et al. 2008a).

For surface reactions where the rate limiting step is adsorption, kinetic expressions based on adsorption isotherms can be used. One of the most commonly used expressions is the Langmuir-Hinshelwood equation.

2.3 Oxidation of UO_2 by radiolytic oxidants

The kinetics for reactions between various oxidants in aqueous solution and UO_2 has been studied for almost half a century. Among the oxidants formed upon water radiolysis, H_2O_2 and O_2 (a secondary product) have attracted most of the attention (Roth and Jonsson 2008). Studies have shown that H_2O_2 is around 200 times more reactive than O_2 towards UO_2 (Shoesmith et al. 1985). Around two decades ago, it was concluded that the rate constant for oxidation of UO_2 in aqueous suspensions is correlated to the one-electron reduction potential of the oxidant through a linear free energy relationship (Ekeroth and Jonsson 2003). On the basis of this relationship, it was possible to estimate the rate constants for species that are more difficult to assess experimentally such as the hydroxyl radical and the carbonate radical anion. For both of these radicals, the reaction was concluded to be diffusion controlled (Ekeroth and Jonsson 2003). Since then, the general mechanism for the reaction with UO_2 has been revised for some of the radiolysis products (Barreiro Fidalgo et al. 2018).

For oxidants that do not have diffusion-controlled rate constants for the reaction with UO_2 (e.g., H_2O_2 and O_2), epsilon particles (noble metal particles consisting of fission products) can catalyze the reaction (Figure 2-1).

2.4 Dissolution of oxidized UO_2

U(VI) formed upon oxidation of UO_2 can dissolve as UO_2^{2+} . In pure water this is a fairly slow process but in groundwater containing complexing agents such as $\text{HCO}_3^-/\text{CO}_3^{2-}$, soluble UO_2^{2+} complexes can be formed which will enhance the rate of dissolution considerably (de Pablo et al. 1999, Hossain et al. 2006). The kinetics of the dissolution process is not straight forward to assess since it is quite difficult to produce controlled amounts of oxidized UO_2 prior to exposure to an aqueous solution. Instead, the dissolution kinetics must be assessed in an oxidative dissolution experiment where oxidation kinetics is also affecting the overall result (Hossain et al. 2006). In solutions where the solubility could be a limiting factor, analyzing dissolution kinetics becomes even more complex.

2.5 The relative impact of radiolytic oxidants

In order to explore the possibility of simplifying numerical modelling of radiation induced dissolution of spent nuclear fuel, the relative impact of the radiolytic oxidants was assessed (Ekeroth et al. 2006). The assessment was based on oxidant concentrations obtained from numerical simulations and rate constants for the different oxidants. The assessment showed that radiation induced oxidation of UO_2 is completely dominated by H_2O_2 in α -irradiated systems. For β - and γ -irradiated systems, H_2O_2 is still the dominating oxidant but other oxidants are also of significance (Ekeroth et al. 2006). The relative impact of the radiolytic oxidants (α -radiolysis) is summarized in the table below.

Table 2-1. Relative impact (in %) of aqueous radiolysis products in α -radiation induced oxidative dissolution of UO₂.

Conditions	H ₂ O ₂	O ₂	O ₂ ^{•-}	HO ₂ [•]	CO ₃ ^{•-}	•OH
Pure water	100.0	0.01	0	0.03	0	0
H ₂ (40 bar)	99.9	0	0	0.02	0	0.03
H ₂ (40 bar) and HCO ₃ ⁻ (10 mM)	100.0	0	0	0	0.02	0
HCO ₃ ⁻ (10 mM)	99.9	0.09	0	0	0	0

2.6 The mechanism of the reaction between H₂O₂ and UO₂

It has long been known that H₂O₂ reacts with UO₂ both by oxidizing the surface and by surface catalyzed decomposition to produce O₂ and H₂O. Earlier, it was assumed that these two competing reactions occur at different surface sites. However, in a relatively recent study it was shown that the two competing reactions share a common intermediate and therefore occur at the same site (Barreiro Fidalgo et al. 2018). The mechanism is described below.



This mechanism was verified by analyzing the impact of H₂O₂ concentration on the dissolution yield (Nilsson and Jonsson 2011), i.e., the ratio between the amount of dissolved uranium and the amount of consumed H₂O₂ (Barreiro Fidalgo et al. 2018). These experiments showed that the dissolution yield decreases with increasing H₂O₂ concentration. The mechanism above accounts for this concentration dependence.

This mechanism also opens up for a number of reactions that have not been considered previously since the surface bound hydroxyl radical (HO[•]—UO₂) is a new species in this context. Solutes reacting with the surface bound hydroxyl radical will have a direct impact on the oxidative dissolution of the UO₂ matrix. Recent experimental studies have shown that the surface bound hydroxyl radical can be scavenged by organic solutes such as Tris and methanol and by Br⁻ (Lousada and Jonsson 2010, Lousada et al. 2013b, Yang and Jonsson 2014, Yang and Jonsson 2015, Toijer and Jonsson 2020, Carlsson et al. 2022). The immediate effect of this is of course that the surface bound hydroxyl radical is scavenged which prevents oxidation as well as catalytic decomposition of H₂O₂ (i.e., the formation of O₂). In some cases, the radical product could contribute further to the surface reactions. In case reducing radicals are formed, they could reduce oxidized surface sites back to U(IV) and thereby further inhibit the oxidative dissolution.

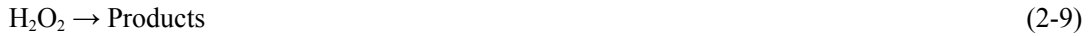
2.7 The effect of H₂

The presence of H₂ from anaerobic corrosion of iron or water radiolysis has been shown to efficiently inhibit oxidative dissolution of UO₂-based spent nuclear fuel. The actual mechanism of this inhibition has been discussed for quite some time. The origin of the H₂ effect can be divided into three parts: (1) Effect of H₂ on radiolytic production of oxidants, (2) Reaction between H₂ and the surface bound hydroxyl radical, and (3) ϵ -particle catalyzed reduction of oxidized uranium on the pellet surface. The first effect is simply a consequence of the overall mechanism for water radiolysis and it is an effect that will never completely suppress the oxidative dissolution (Trummer and Jonsson 2010). The second effect is at the moment more of a postulated effect attributed to the mechanism for the reaction between H₂O₂ and UO₂. It is reasonable to believe that the surface bound hydroxyl radical can react with H₂. This would prevent oxidation but also produce a reducing hydrogen atom capable of reducing oxidized uranium on the surface. This mechanism would account for observations made on pure UO₂ where fission products are not present (Bauhn et al. 2018, Hansson et al. 2021, Hansson and Jonsson 2023).

In general, this mechanism has a larger impact on the dissolution than the purely radiolytic effect. The third effect, ϵ -particle catalyzed reduction of oxidized uranium, has been studied quite extensively using various methods. Electrochemical methods have demonstrated that the electrochemical potential of a UO_2 electrode in an electrolyte containing dissolved H_2 is significantly lower if the UO_2 electrode contains noble metal inclusions compared to if it is pure UO_2 (Broczkowski et al. 2005). Kinetic studies have shown that this process is very fast and that the rate limiting step, the reaction between H_2 and the ϵ -particle, is diffusion controlled (Trummer et al. 2008). The reduction of oxidized uranium on the surface competes with the dissolution of the same species and as soon as the reduction reaction becomes faster than the dissolution reaction, the oxidative dissolution becomes completely inhibited. It has been shown that this process becomes very efficient already at fairly low H_2 -concentrations (Eriksen and Jonsson 2007).

2.8 Other reactions catalyzed by ϵ -particles

Noble metal particles have been found to catalyze a number of other reactions of relevance in radiation induced oxidative dissolution of UO_2 -based nuclear fuel (Nilsson and Jonsson 2008a, Nilsson and Jonsson 2008b, Maier and Jonsson 2019). The most relevant reactions known and explored so far are the following:



These reactions have been studied using Pd-particles. For the reduction reactions (2-7) and (2-8) it has previously been shown that the kinetics is independent of the partial pressure of H_2 above 1 bar (Nilsson and Jonsson 2008a, Nilsson and Jonsson 2008b). Under these conditions, the kinetic expression can be written as Equation (2-2) above. The reason for the H_2 -pressure independence is that the encounter between H_2O_2 or UO_2^{2+} and the Pd-particle is the rate determining step. More recently, these reactions have been studied at lower H_2 pressures (Maier and Jonsson 2019). In both cases, H_2 -pressure dependence is observed. However, in the case of UO_2^{2+} reduction, the pressure dependence on the kinetics cannot be quantified due to experimental artifacts. For this reaction, a lag-phase is observed at low H_2 -pressures. The lag-phase increases with decreasing H_2 -pressure and was argued to be attributed to the presence of O_2 in the initial reaction mixture (originating from an aqueous UO_2^{2+} solution injected at the start of the experiment). Interestingly, the rate of UO_2^{2+} reduction differs very little between the H_2 -pressures once the lag-phase is over. It is therefore reasonable to use the kinetic expression from Equation (2-2) for this reaction. The rate constant has been determined to $1.5 \times 10^{-5} \text{ m s}^{-1}$ (Nilsson and Jonsson 2008b).

For the reduction of H_2O_2 at low H_2 -pressures it was found that the pressure dependence could be described using the Langmuir isotherm. The kinetics could then be described using Langmuir-Hinshelwood kinetics. The resulting expression is given below:

$$-\frac{d[\text{H}_2\text{O}_2]}{dt} = k_2[\text{H}_2\text{O}_2] \frac{SA}{V} \theta \quad (2-10)$$

where θ is the fractional surface coverage of H_2 given by the Langmuir isotherm:

$$\theta = \frac{K[\text{H}_2]}{K[\text{H}_2]+1} \quad (2-11)$$

The equilibrium constant, K , was found to be $8.1 \times 10^4 \text{ M}^{-1}$ and the rate constant in Equation (2-10), k_2 , was found to be $2.4 \times 10^{-5} \text{ m s}^{-1}$ (Maier and Jonsson 2019).

The mechanism of the catalytic decomposition of H_2O_2 on Pd was investigated using radical scavengers to verify the existence of reactive intermediates. The expected mechanism was that of catalytic decomposition on oxide surfaces with the intermediate formation of surface-bound hydroxyl radicals. For oxide surfaces in general, this mechanism has been verified by using Tris or methanol for which the product after reaction with the hydroxyl radical is formaldehyde (Lousada et al. 2013a, Yang and Jonsson 2014, Yang and Jonsson 2015). More recently, the mechanism was also confirmed using

coumarin as radical scavenger (Leandri et al. 2019, Maier et al. 2019). One of the products formed upon reaction with the hydroxyl radical is fluorescent and readily detectable. Quite unexpectedly, surface-bound hydroxyl radicals could not be confirmed as intermediates of the catalytic decomposition of H_2O_2 on Pd. The overall second order rate constant for the catalytic decomposition of H_2O_2 on Pd was determined to $4.95 \times 10^{-6} \text{ m s}^{-1}$ (Maier and Jonsson 2019).

3 The steady-state approach

In any aqueous system exposed to ionizing radiation with a constant dose rate distribution, the rate of production of radiolysis products in the aqueous phase will at some point be balanced by the rate of consumption of the same product. At this point, steady-state has been reached and the concentration of the radiolysis product in question will be constant. For the radical species, such as HO·, CO₃^{·-}, H·, HO₂[·]/O₂⁻ and e_{aq}⁻, the steady-state concentrations will be very low. However, for molecular products such as H₂O₂, O₂ and H₂, the steady-state concentrations can be considerably higher. The processes consuming the radiolysis products in the repository case could be reactions with the fuel surface, reactions with solutes, reactions with other solid surfaces or diffusion out of the canister. This means that the maximum rate of fuel oxidation by a radiolytic oxidant is equal to the rate of radiolytic production of the same oxidant. This constitutes the most conservative case for a safety assessment.

Previous studies based on numerical simulations of a fuel-water system taking the spatial dose rate distribution and diffusion into account showed that the surface concentration of H₂O₂ rapidly reached the overall system steady-state level even though it takes time to reach the homogeneous system steady-state (Nielsen and Jonsson 2008, Nielsen et al. 2008a, Nielsen et al. 2008b). As the surface concentration of H₂O₂ is what controls the rate of UO₂ oxidation, it was concluded that a steady-state approach could be used to simulate radiation induced oxidative dissolution of UO₂-based spent nuclear fuel. The rate of UO₂ oxidation is then given by the following expression:

$$r_{ox} = r_{H_2O_2} = \int_{x=0}^{x_{max}} D(x) \times \rho \times G(H_2O_2) dx \quad (3-1)$$

In this expression r_{ox} denotes the rate of UO₂ oxidation (in mol m⁻² s⁻¹), $r_{H_2O_2}$ the rate of radiolytic H₂O₂ production (in mol m⁻² s⁻¹), $\dot{D}(x)$ the α -dose rate at distance x from the surface, ρ the density of water and $G(H_2O_2)$ the radiation chemical yield for H₂O₂ under α -radiolysis. Instead of integrating the dose rate profile from the surface to the distance corresponding to the maximum range of the α -particles, the average dose rate can be used. The expression is then simplified to:

$$r_{ox} = r_{H_2O_2} = \overline{D(x)} \times \rho \times G(H_2O_2) \times x_{max} \quad (3-2)$$

Using the steady-state approach, it is also possible to account for the ϵ -particle catalyzed H₂-effect (Jonsson et al. 2007). By multiplying the rate constant for the reaction between H₂ and the ϵ -particle with the concentration of H₂ and the fractional surface coverage of ϵ -particles (ϵ_{rel}), the maximum rate of reduction is obtained (in reality it is impossible to reduce more than what has been oxidized). The net rate of UO₂ dissolution is then given by the difference between the rate of oxidant production and the maximum rate of U(VI)-reduction (Jonsson et al. 2007):

$$r_{diss} = r_{ox} - k_{H_2}[H_2]\epsilon_{rel} \quad (3-3)$$

As the maximum rate of U(VI)-reduction can be larger than the rate of oxidant formation under certain conditions, it is important to keep in mind that the net rate of fuel oxidation cannot be lower than 0.

The steady-state approach can be used to benchmark new modelling approaches as it provides an upper limit for the rate of radiation induced oxidative dissolution of UO₂ (Eriksen et al. 2012).

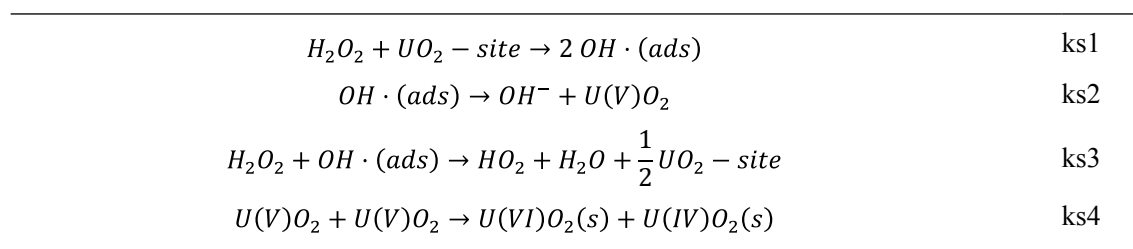
4 Reactions and rate constants

The rate constants for the reactions discussed above are presented below. For practical purposes (mainly to allow surface sites to be consumed or blocked through the various reactions) it is advisable to convert solid surface area to solution volume ratios to surface site concentrations. This can be done by using the surface site density. The surface site concentration is obtained by multiplying the solid surface area to solution volume ratio with the surface site density. The rate constant must then be divided with the surface site density. For UO_2 , the surface site density has been determined to be $2.1 \times 10^{-4} \text{ mol} \cdot \text{m}^{-2}$ (Hossain and Jonsson 2008).

4.1 $H_2O_2 + UO_2$

The mechanism for the reaction between H_2O_2 and UO_2 is described above (Barreiro Fidalgo et al. 2018). Given its complexity, it is not possible to experimentally assess the rate constants of the elementary reactions separately from each other. However, on the basis of experiments performed at different initial concentrations of H_2O_2 at a given solid surface to solution volume ratio where the concentrations of H_2O_2 and dissolved uranium were monitored as a function of time, the individual rate constants can be assessed using numerical fitting to the mechanism (Hansson et al. 2023). It should be noted the reaction between two HO_2^{\cdot} producing H_2O_2 and O_2 is already known and therefore does not require fitting. For modelling purpose, it is also important to include a pathway to production of U(VI) as this is the species that will eventually be dissolved. This is done by introducing a disproportionation reaction between two U(V) to produce U(IV) and U(VI).

The reaction between H_2O_2 and UO_2 is described as follows in the model:

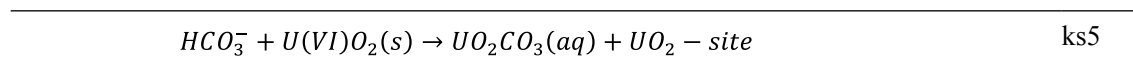


Based on fitting to experimental data, the rate constants were determined to $ks1 = 0.462 \text{ M}^{-1} \text{ s}^{-1}$, $ks2 = 0.191 \text{ s}^{-1}$, $ks3 = 197 \text{ M}^{-1} \text{ s}^{-1}$ and $ks4 = 34.1 \text{ M}^{-1} \text{ s}^{-1}$.

It should be noted that these rate constants were derived on the basis of experimental data on powder suspensions.

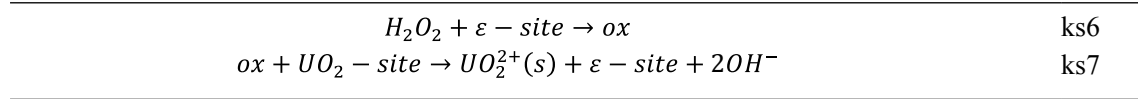
4.2 HCO_3^- facilitated dissolution of UO_2^{2+}

The dissolution of UO_2^{2+} in carbonate solution has been found to be close to diffusion controlled (Hossain et al. 2006). Therefore, we set the value for $ks5 = 10^3 \text{ M}^{-1} \cdot \text{s}^{-1}$ which corresponds to diffusion controlled in this particular heterogeneous system (i.e., a powder suspension) (Hansson and Jonsson 2023). The reaction can be expressed as follows:



4.3 H₂O₂ + UO₂ catalyzed by ε-particles

Work on Pd-containing UO₂ pellets showed that the noble metal catalyzed oxidation of U(IV) by H₂O₂ has a rate constant 100 times higher than that of the direct reaction between H₂O₂ and UO₂ (Trummer et al. 2009). The rate determining step is the reaction between H₂O₂ and the ε-particles and therefore the kinetics can be described as the heterogeneous version of a bimolecular reaction. To translate this into the rate of UO₂ oxidation we must include an additional reaction where the oxidant-equivalent formed in the reaction between H₂O₂ and the ε-particle (“ox”) oxidizes UO₂ to U(VI) (Hansson and Jonsson 2023). The latter reaction should have a rate constant high enough not to affect the oxidation of UO₂ but low enough not to cause numerical problems. This is a way to avoid third order kinetics for which the rate constants are not known.

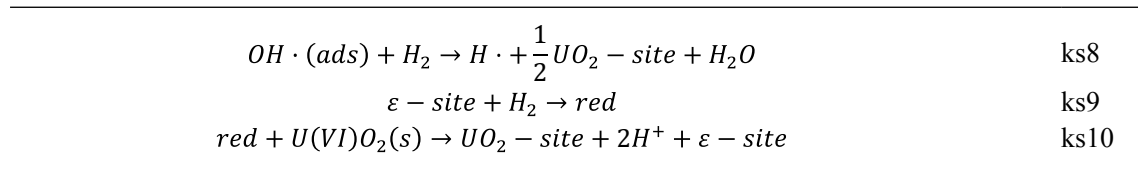


For this reason, ks6 is set to 100 times that of ks1 (i.e., ks6 = 46.2 M⁻¹ s⁻¹). A value of ks7 = 10¹⁶ M⁻¹ s⁻¹ was found to satisfy the boundary conditions mentioned above.

4.4 The interfacial H₂ effect

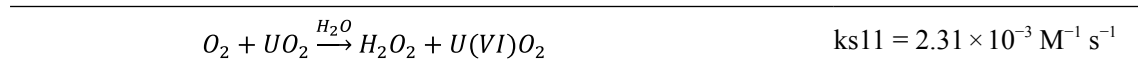
The rate constant for the reaction between H₂ and the surface-bound hydroxyl radical is not known experimentally. However, from homogeneous reactions in solution we know that the rate constant for the reaction between the hydroxyl radical and H₂ is more or less the same as the rate constant for the reaction between the hydroxyl radical and H₂O₂ (Jonsson 2022). Consequently, ks8 could be set equal to ks3. However, the surface-bound hydroxyl radical has been shown to be considerably less reactive than the free hydroxyl radical (Yang and Jonsson 2015, Toijer and Jonsson 2020, Carlsson et al. 2022). The reduction potential of the surface-bound hydroxyl radical is more than 300 mV lower than for the free hydroxyl radical (Lawless et al. 1991). This would imply that hydrogen abstraction from H₂ would not be a spontaneous reaction for the surface-bound hydroxyl radical while hydrogen abstraction from H₂O₂ still would be. Hence, it is likely that ks8 is considerably lower than ks3. A value between 50 and 100 M⁻¹ s⁻¹ appears reasonable based on previous simulations.

Experimental work on UO₂ pellets containing Pd-particles to mimic the effects of noble metal inclusions have shown that the reaction between H₂ and the noble metal inclusions is close to diffusion controlled (Trummer et al. 2008). In other words, ks9 should be close to 10³ M⁻¹ s⁻¹. As in the case of ε-particle catalyzed oxidation of UO₂, the subsequent reaction between “red” and U(VI) should have a rate constant high enough not to affect the reduction of U(VI) but low enough not to cause numerical problems. A value of ks10 = ks7 = 10¹⁶ M⁻¹·s⁻¹ was found to satisfy these boundary conditions.



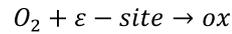
4.5 O₂ + UO₂

As mentioned above, O₂ is less reactive towards UO₂ than H₂O₂ by approximately a factor of 200 (Shoesmith et al. 1985). This implies that the rate constant should be ks11 = ks1/200 = 2.31 × 10⁻³ M⁻¹ s⁻¹.



4.6 O₂ + UO₂ catalyzed by ε-particles

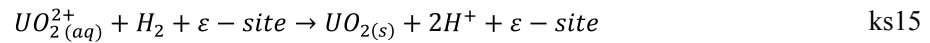
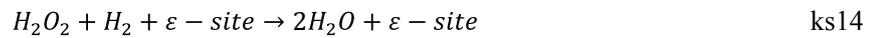
The ε-particle catalyzed reaction between O₂ and UO₂ has been shown to be roughly a factor of 60 lower than the corresponding reaction for H₂O₂ (Trummer et al. 2009). The rate constant is consequently ks12 = ks6/60 = 0.77 M⁻¹ s⁻¹.



$$ks12 = 0.77 \text{ M}^{-1} \text{ s}^{-1}$$

4.7 Other reactions catalyzed by ε-particles

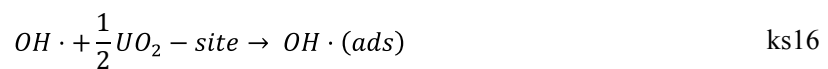
The additional reactions catalyzed by noble metal particles are the following (Nilsson and Jonsson 2008a, Nilsson and Jonsson 2008b, Maier and Jonsson 2019):



The second order rate constants for the noble metal catalyzed reactions between H₂ and dissolved UO₂²⁺ or H₂O₂ and the noble metal catalyzed decomposition of H₂O₂ are given in the unit m s⁻¹. To convert the rate constants to the same units as was used for the other surface reactions (i.e., M⁻¹ s⁻¹), the rate constants in m s⁻¹ must be divided by the surface site density. It should be kept in mind that the surface site density that should be used for the above reactions refers to UO₂ and not to Pd. However, this is of minor importance since we are essentially using the solid surface area to solution volume ratio as our basic parameter to quantify the amount of reactive surface. For the noble metal-catalyzed reactions we should use the overall UO₂ surface area to solution volume ratio multiplied with the fractional coverage of noble metal particles. The resulting rate constants are: ks13 = 23.6 M⁻¹ s⁻¹, ks14 = 114 M⁻¹ s⁻¹ and ks15 = 71.4 M⁻¹ s⁻¹. It must be kept in mind that for ks14 a Langmuir-Hinshelwood-type of kinetic expression must be used (Maier and Jonsson 2019).

4.8 Reactions of ·OH and CO₃^{·-} with UO₂

As stated above, both ·OH and CO₃^{·-} are expected to react with UO₂ with diffusion-controlled rate constants (Ekeröth and Jonsson 2003). The reactions can be described as follows:



The rate constants ks16 and ks17 are both estimated to be diffusion controlled, 10³ M⁻¹ s⁻¹ (Ekeröth and Jonsson 2003, Hansson and Jonsson 2023).

4.9 Summary of reactions and rate constants

$H_2O_2 + UO_2 - site \rightarrow 2 OH \cdot (ads)$	ks1 = 0.462 M ⁻¹ s ⁻¹
$OH \cdot (ads) \rightarrow OH^- + U(V)O_2$	ks2 = 0.191 s ⁻¹
$H_2O_2 + OH \cdot (ads) \rightarrow HO_2 + H_2O + \frac{1}{2} UO_2 - site$	ks3 = 197 M ⁻¹ s ⁻¹
$U(V)O_2 + U(V)O_2 \rightarrow U(VI)O_2(s) + U(IV)O_2(s)$	ks4 = 34.1 M ⁻¹ s ⁻¹
$HCO_3^- + U(VI)O_2(s) \rightarrow UO_2CO_3(aq) + UO_2 - site$	ks5 = 10 ³ M ⁻¹ s ⁻¹
$H_2O_2 + \varepsilon - site \rightarrow ox$	ks6 = 46.2 M ⁻¹ s ⁻¹
$ox + UO_2 - site \rightarrow UO_2^{2+}(s) + \varepsilon - site + 2OH^-$	ks7 = 10 ¹⁶ M ⁻¹ s ⁻¹
$OH \cdot (ads) + H_2 \rightarrow H \cdot + \frac{1}{2} UO_2 - site + H_2O$	ks8 = 50–100 M ⁻¹ s ⁻¹
$\varepsilon - site + H_2 \rightarrow red$	ks9 = 10 ³ M ⁻¹ s ⁻¹
$red + U(VI)O_2(s) \rightarrow UO_2 - site + 2H^+ + \varepsilon - site$	ks10 = 10 ¹⁶ M ⁻¹ s ⁻¹
$O_2 + UO_2 \xrightarrow{H_2O} H_2O_2 + U(VI)O_2$	ks11 = 2.31 × 10 ⁻³ M ⁻¹ s ⁻¹
$O_2 + \varepsilon - site \rightarrow ox$	ks12 = 0.77 M ⁻¹ s ⁻¹
$H_2O_2 + \varepsilon - site \rightarrow H_2O + \frac{1}{2} O_2$	ks13 = 23.6 M ⁻¹ s ⁻¹
$H_2O_2 + H_2 + \varepsilon - site \rightarrow 2H_2O + \varepsilon - site$	ks14 ^a = 114 M ⁻¹ s ⁻¹
$UO_2^{2+}(aq) + H_2 + \varepsilon - site \rightarrow UO_2(s) + 2H^+ + \varepsilon - site$	ks15 = 71.4 M ⁻¹ s ⁻¹
$OH \cdot + \frac{1}{2} UO_2 - site \rightarrow OH \cdot (ads)$	ks16 = 10 ³ M ⁻¹ s ⁻¹
$CO_3^{2-} + \frac{1}{2} UO_2 - site \rightarrow U(V)O_2$	ks17 = 10 ³ M ⁻¹ s ⁻¹

^a The rate expression for H₂O₂ consumption is the following:

$-\frac{d[H_2O_2]}{dt} = ks14[H_2O_2] \frac{8.1 \times 10^4 [H_2]}{8.1 \times 10^4 [H_2] + 1} \times SC$ where SC is the surface site concentration derived from the solid surface area to solution volume ratio and the site density derived for UO₂.

5 Known unknowns

The reaction mechanisms, rate expressions and rate constants presented above could be seen as the state-of-the-art at the time when this report was published. However, this set of data is by no means complete and we can already identify a number of known unknowns that we must focus our attention on to develop numerical models for radiation induced oxidative dissolution of UO_2 -based spent nuclear fuel further. The known knowledge gaps are briefly summarized below:

5.1 Transferring kinetics from powder to pellet

The majority of the kinetic data available today come from experiments performed on UO_2 -powder suspensions (stoichiometric or hyperstoichiometric) (Roth and Jonsson 2008). As mentioned above, the size of the solid objects involved in the heterogeneous reaction is of key-importance (Jonsson 2010). It is therefore very important to derive rate constants for pellets rather than powders. Admittedly, this is not straightforward as it is much more difficult to vary the solid surface area to solution volume ratio when pellets are used. Transferring kinetics from powder to pellet can to some extent be based on kinetic theory (Jonsson 2010) but this should be complemented by control experiments to validate any assumptions that are made.

5.2 Extended exposure

In powder experiments the exposed surface area is in general very large and during an experiment the exposure to oxidants per surface area of material is very low. Experiments on pellets where the exposure to oxidants per surface area is considerably higher have shown that the behaviour of the material changes with exposure (Maier et al. 2020a, Maier et al. 2020b). In general, the so-called dissolution yield (Nilsson and Jonsson 2011) which is given by the ratio between the amount of dissolved uranium and consumed hydrogen peroxide reflects the competition between oxidation of UO_2 and catalytic decomposition of H_2O_2 on the UO_2 surface. Pellet experiments with variable exposure to H_2O_2 and 10 mM HCO_3^- solutions have clearly shown that the dissolution yield decreases with increasing exposure (Maier et al. 2020a, Maier et al. 2020b). The dissolution yield for pellets is also significantly lower than the dissolution yield for powder. In other words, the ratio between the rate constants for oxidation and catalytic decomposition is different for pellets compared to powder and may even change with exposure for pellets. This must be better understood and should also be accounted for in the model.

5.3 Secondary phases

Secondary phases such as studtite could be formed on the UO_2 surface and alter the reactivity of the fuel (Li et al. 2020, Li et al. 2021, Li et al. 2022). Other secondary phases may also form in the repository. Although the dynamics and spatial location of such a process are very difficult to predict, it would be desirable to include the kinetics for secondary phase formation and dissolution in the model. Presently, more kinetic data on studtite formation as well as studtite and meta-studtite dissolution under various conditions are becoming available.

5.4 Speciation in solution

It has been known for quite some time that the radiolysis product H_2O_2 can form ternary complexes with UO_2^{2+} and $\text{HCO}_3^-/\text{CO}_3^{2-}$ (Zanonato et al. 2012a, Zanonato et al. 2012b). Recent studies have shown that the speciation of H_2O_2 (i.e., whether it is free or complexed) has a major impact on the kinetics of UO_2 oxidation (Olsson et al. 2022). Also, in systems with high salinity, H_2O_2 and UO_2^{2+}

can form ternary complexes with Cl^- and Br^- which also affects the kinetics of UO_2 oxidation (El Jamal et al. 2021, Li et al. 2022). It is important to note that the ternary complexes become particularly important at higher UO_2^{2+} concentrations. It would therefore be very useful to perform speciation calculations for UO_2^{2+} concentrations that are deemed to be reasonable under repository conditions. If such calculations would show that a significant fraction of the H_2O_2 is present as ternary complex, the kinetic model should be complemented with a module for speciation calculations.

5.5 Kinetic expressions based on adsorption isotherms

Traditionally, the kinetic expressions used for reactions between radiolytic oxidants and the UO_2 surface have been of the type described in Equation (2-2) above. More recent studies indicate that simple second order kinetics may not always perfectly reproduce the experimental results (Barreiro Fidalgo et al. 2018, Olsson et al. 2022). In such cases, rate expressions based on adsorption isotherms appear to be more appropriate. This is particularly true for H_2O_2 . More efforts should be made in order to analyze kinetic data in terms of adsorption isotherms and, if possible, include these isotherms in the general kinetic model. Most probably, a kinetic expression based on an isotherm for H_2O_2 can be presented in the near future.

5.6 Impact of interfacial G-values

Numerous studies have shown that the radiation chemical yield close to a solid surface or in confined volumes can differ significantly from the corresponding values in bulk water (LaVerne and Tandon 2002). Most of these studies focus on H_2 for which much higher G-values are in general observed close to a solid surface. Whether this would have an impact or not on radiation induced dissolution of UO_2 -based nuclear fuel needs to be assessed. If deemed important, attempts should be made to incorporate interfacial G-values in the simulations.

5.7 Surface reactivity of reducing radicals

Reducing radicals such as H^\cdot and e_{aq}^- are usually not considered when simulating the rate of oxidative dissolution of UO_2 . Even if the reactivity of these radicals is low towards U(IV) , they most probably display higher reactivity towards U(V) and U(VI) present on the surface. The rate constants of these reactions need to be experimentally assessed. In addition, their potential impact could be explored using the numerical model and the fact that the rate constants cannot exceed diffusion-control.

References

SKB's (Svensk Kärnbränslehantering AB) publications can be found at www.skb.com/publications.

- Barreiro Fidalgo A, Kumagai Y, Jonsson M, 2018.** The role of surface-bound hydroxyl radicals in the reaction between H_2O_2 and UO_2 . *Journal of Coordination Chemistry* 71, 1799–1807.
- Bauhn L, Hansson N, Ekberg C, Fors P, Delville R, Spahiu K, 2018.** The interaction of molecular hydrogen with α -radiolytic oxidants on a (U,Pu) O_2 surface. *Journal of Nuclear Materials* 505, 54–61.
- Broczkowski M, Noël J, Shoesmith D, 2005.** The inhibiting effects of hydrogen on the corrosion of uranium dioxide under nuclear waste disposal conditions. *Journal of Nuclear Materials* 346, 16–23.
- Carlsson C, Fégeant B, Svensson E, Wiklund L, Jonsson M, 2022.** On the Selectivity of Radical Scavengers Used to Probe Hydroxyl Radical Formation in Heterogeneous Systems. *The Journal of Physical Chemistry* 126, 12435–12440.
- de Pablo J, Casas I, Giménez J, Molera M, Rovira M, Duro L, Bruno J, 1999.** The oxidative dissolution mechanism of uranium dioxide. I. The effect of temperature in hydrogen carbonate medium. *Geochimica et Cosmochimica Acta* 63, 3097–3103.
- Ekeroth E, Jonsson M, 2003.** Oxidation of UO_2 by radiolytic oxidants. *Journal of Nuclear Materials* 322, 242–248.
- Ekeroth E, Roth O, Jonsson M, 2006.** The relative impact of radiolysis products in radiation induced oxidative dissolution of UO_2 . *Journal of Nuclear Materials* 355, 38–46.
- El Jamal G, Li J, Jonsson M, 2021.** H_2O_2 -Induced Oxidative Dissolution of UO_2 in Saline Solutions. *European Journal of Inorganic Chemistry* 40, 4146–4237.
- Eriksen T E, Jonsson M, 2007.** The effect of hydrogen on dissolution of spent fuel in $0.01 \text{ mol} \times \text{dm}^{-3}$ NaHCO_3 solution. SKB TR-07-06, Svensk Kärnbränslehantering AB.
- Eriksen T E, Shoesmith D W, Jonsson M, 2012.** Radiation induced dissolution of UO_2 based nuclear fuel – A critical review of predictive modelling approaches. *Journal of Nuclear Materials* 420, 409–423.
- Grenthe I, Ferri D, Salvatore F, Riccio G, 1984.** Studies on metal carbonate equilibria. Part 10. A solubility study of the complex formation in the uranium(VI)-water-carbon dioxide (g) system at 25 °C. *Journal of the Chemical Society, Dalton Transactions* 11, 2439–2443.
- Hansson N L, Jonsson M, 2023.** Exploring H_2 -effects on radiation-induced oxidative dissolution of UO_2 -based spent nuclear fuel using numerical simulations. *Radiation Physics and Chemistry* 210, 111055.
- Hansson N, Tam P, Ekberg C, Spahiu K, 2021.** XPS study of external α -radiolytic oxidation of UO_2 in the presence of argon or hydrogen. *Journal of Nuclear Materials* 543, 152604.
- Hansson N, Jonsson M, Ekberg C, Spahiu K, 2023.** Modelling radiation-induced oxidative dissolution of UO_2 -based spent nuclear fuel on the basis of the hydroxyl radical mediated surface mechanism: Exploring the impact of surface reaction mechanism and spatial and temporal resolution. *Journal of Nuclear Materials* 578, 154369.
- Hossain M M, Jonsson M, 2008.** UO_2 oxidation site densities determined by one- and two-electron oxidants. *Journal of Nuclear Materials* 373, 186–189.
- Hossain M M, Ekeroth E, Jonsson M, 2006.** Effects of HCO_3^- on the kinetics of UO_2 oxidation by H_2O_2 . *Journal of Nuclear Materials* 358, 202–208.
- Jonsson M, 2010.** Radiation-Induced Processes at Solid-Liquid Interfaces. In *Recent Trends in Radiation Chemistry*. In Wishart J F, Rao B S M (eds). *Recent Trends in Radiation Chemistry*. Singapore: World Scientific, 301–324.
- Jonsson M, 2022.** Assessment of homogeneous processes and parameters to be used in models for radiation induced dissolution of spent nuclear fuel. SKB R-22-06, Svensk Kärnbränslehantering AB.

- Jonsson M, Nielsen F, Roth O, Ekeroth E, Nilsson S, Hossain M M, 2007.** Radiation Induced Spent Nuclear Fuel Dissolution under Deep Repository Conditions. *Environmental Science & Technology* 41, 7087–7093.
- LaVerne J A, Tandon L, 2002.** H₂ Production in the Radiolysis of Water on CeO₂ and ZrO₂. *The Journal of Physical Chemistry B* 106, 380–386.
- Lawless D, Serpone N, Meisel D, 1991.** Role of OH[·] Radicals and Trapped Holes in Photocatalysis. A Pulse Radiolysis Study. *Journal of Physical Chemistry* 95, 5166–5170.
- Leandri V, Gardner J M, Jonsson M, 2019.** Coumarin as a Quantitative Probe for Hydroxyl Radical Formation in Heterogeneous Photocatalysis. *Journal of Physical Chemistry C* 123, 6667–6674.
- Li J, Maier A C, Jonsson M, 2020.** Stability of Studtite in Aqueous Suspension: Impact of HCO₃⁻ and Ionizing Radiation on the Dynamics of Dissolution. *ACS Applied Energy Materials* 3, 352–357.
- Li J, Szabó Z, Jonsson M, 2021.** Meta-studtite stability in aqueous solutions. Impact of HCO₃⁻, H₂O₂ and ionizing radiation on dissolution and speciation. *Dalton Transactions* 50, 6568–6577.
- Li J, Szabó Z, Jonsson M, 2022.** Stability of Studtite in Saline Solution: Identification of Uranyl- Peroxo-Halo Complex. *Inorganic Chemistry* 61, 8455–8466.
- Lousada C M, Jonsson M, 2010.** Kinetics, Mechanism, and Activation Energy of H₂O₂ Decomposition on the Surface of ZrO₂. *The Journal of Physical Chemistry C* 114, 11202–11208.
- Lousada C M, Yang M, Nilsson K, Jonsson M, 2013a.** Catalytic decomposition of hydrogen peroxide on transition metal and lanthanide oxides. *Journal of Molecular Catalysis A: Chemical* 379, 178–184.
- Lousada C M, LaVerne J A, Jonsson M, 2013b.** Enhanced hydrogen formation during the catalytic decomposition of H₂O₂ on metal oxide surfaces in the presence of HO radical scavengers. *Physical Chemistry Chemical Physics* 30, 12674–12679.
- Maier A C, Jonsson M, 2019.** Pd-Catalyzed Surface Reactions of Importance in Radiation Induced Dissolution of Spent Nuclear Fuel Involving H₂. *ChemCatChem* 11, 5108–5115.
- Maier A C, Hercegljija Iglebaek E, Jonsson M, 2019.** Confirming the Formation of Hydroxyl Radicals in the Catalytic Decomposition of H₂O₂ on Metal Oxides Using Coumarin as a Probe. *ChemCatChem* 11, 5435–5438.
- Maier A C, Barreiro Fidalgo A, Jonsson M, 2020a.** Impact of H₂ on Consecutive H₂O₂ Exposures on the Oxidative Dissolution of (U_{1-x}Gd_x)O₂ Pellets Under Deep Repository Conditions for Spent European Journal of Inorganic Chemistry 20, 1946–1950.
- Maier A C, Kegler P, Klinkenberg M, Baena A, Finkeldei S, Brandt F, Jonsson M, 2020b.** On the change in UO₂ redox reactivity as a function of H₂O₂ exposure. *Dalton Transactions* 4, 1241–1248.
- Nielsen F, Jonsson M, 2008.** Simulations of H₂O₂ concentration profiles in the water surrounding spent nuclear fuel taking mixed radiation fields and bulk reactions into account. *Journal of Nuclear Materials* 374, 281–285.
- Nielsen F, Lundahl K, Jonsson M, 2008a.** Simulations of H₂O₂ concentration profiles in water surrounding spent nuclear fuel. *Journal of Nuclear Materials* 372, 32–35.
- Nielsen F, Ekeroth E, Eriksen T E, Jonsson M, 2008b.** Simulation of radiation induced dissolution of spent nuclear fuel using the steady-state approach. A comparison to experimental data. *Journal of Nuclear Materials* 374, 286–289.
- Nilsson S, Jonsson M, 2008a.** On the catalytic effects of UO₂(s) and Pd(s) on the reaction between H₂O₂ and H₂ in aqueous solution. *Journal of Nuclear Materials* 372, 160–163.
- Nilsson S, Jonsson M, 2008b.** On the catalytic effect of Pd(s) on the reduction of UO₂²⁺ with H₂ in aqueous solution. *Journal of Nuclear Materials* 374, 290–292.
- Nilsson S, Jonsson M, 2011.** H₂O₂ and radiation induced dissolution of UO₂ and SIMFUEL pellets. *Journal of Nuclear Materials* 410, 89–93.
- Olsson D, Li J, Jonsson M, 2022.** Kinetic Effects of H₂O₂ Speciation on the Overall Peroxide Consumption at UO₂-Water Interfaces. *ACS Omega* 7, 15929–15935.

- Roth O, Jonsson M, 2008.** Oxidation of $\text{UO}_2(\text{s})$ in aqueous solution. *Central European Journal of Chemistry* 6, 1–14.
- Shoesmith D W, 2000.** Fuel corrosion processes under waste disposal conditions. *Journal of Nuclear Materials* 282, 1–3.
- Shoesmith D W, Sunder S, Johnson L H, Bailey M G, 1985.** Oxidation of Candu UO_2 Fuel by the Alpha-Radiolysis Products of Water. *MRS Online Proceedings Library* 50, 309–316.
- Spinks J W T, Woods R J, 1990.** *An Introduction to Radiation Chemistry*, 3rd ed. New York, NY: John-Wiley and Sons Inc.
- Toijer E, Jonsson M, 2020.** Anion effects on the catalytic decomposition of H_2O_2 on $\text{ZrO}_2(\text{s})$ in aqueous systems. *ChemistrySelect* 5, 13417–13779.
- Trummer M, Jonsson M, 2010.** Resolving the H_2 effect on radiation induced dissolution of UO_2 -based spent nuclear fuel. *Journal of Nuclear Materials* 396, 163–169.
- Trummer M, Nilsson S, Jonsson M, 2008.** On the effects of fission product noble metal inclusions on the kinetics of radiation induced dissolution of spent nuclear fuel. *Journal of Nuclear Materials* 378, 55–59.
- Trummer M, Roth O, Jonsson M, 2009.** H_2 inhibition of radiation induced dissolution of spent nuclear fuel. *Journal of Nuclear Materials* 383, 226–230.
- Yang M, Jonsson M, 2014.** Evaluation of the O_2 and pH Effects on Probes for Surface Bound Hydroxyl Radicals. *The Journal of Physical Chemistry C* 118, 7971–7979.
- Yang M, Jonsson M, 2015.** Surface reactivity of hydroxyl radicals formed upon catalytic decomposition of H_2O_2 on ZrO_2 . *Journal of Molecular Catalysis A: Chemical* 400, 49–55.
- Zanonato P L, Di Bernardo P, Grenthe I, 2012a.** Chemical equilibria in the binary and ternary uranyl(VI)-hydroxide-peroxide systems. *Dalton Transactions* 41, 3380–3386.
- Zanonato P L, Di Bernardo P, Szabó Z, Grenthe I, 2012b.** Chemical equilibria in the uranyl(VI)-peroxide-carbonate system; identification of precursors for the formation of poly-peroxometallates. *Dalton Transactions* 41, 11635–11641.

SKB is responsible for managing spent nuclear fuel and radioactive waste produced by the Swedish nuclear power plants such that man and the environment are protected in the near and distant future.

skb.se